

Examining and calculation of non-classical in the solutions to the true elastic cable under concentrated loads in nanofilm

A. Oveysi Sarabi^{*}; A. Ghanbari

Department of Mechanical Engineering, East Azerbaijan Science and Research Branch,
Islamic Azad University, Tabriz, Iran.

Received 26 February 2015; revised 15 May 2015; accepted 06 June 2015; available online 20 July 2015

ABSTRACT: Due to high surface-to-volume ratio of nanoscale structures, surface stress effects have a significant influence on their behavior. In this paper, a two-dimensional problem for an elastic layer that is bonded to a rigid substrate and subjected to an inclined concentrated line load acting on the surface of the layer is investigated based on Gurtin-Murdoch continuum model to consider surface stress effects. Fourier integral transforms are used to solve the non-classical boundary-value problem related to inclined point load and an analytical solution is obtained for the corresponding boundary-value problem. Selected numerical results are presented for different values of loading angle and are compared with the classical ones to illustrate the influence of the surface stress effects on the stiffness of nano-coating and ultra-thin films. It is found that the surface stress effects have a quite large influence on the response of the nanofilm especially for more vertical loading (higher values of the angle of loading) and make the layer stiffer than the classical case.

Keywords: Boundary-value problem; Elasticity; Nanomechanics; Point loading; Surface stress.

INTRODUCTION

Nanoscience and nanotechnology have generated considerable interest and have attracted much investment in order to develop new revolutionary applications in a wide range of disciplines. To successfully design and manufacture the nanostructures and systems, a fundamental study of their mechanical behavior is essential. Nanomechanics are the area of mechanics in which the mechanical properties and behavior of materials and structures at the nanoscale are studied.

An interesting class of problems in nanoscale mechanics deals with exceptional response and properties due to surface energy effects. These effects can be more substantial especially for thin films where there are a great number of atoms near the surface in comparison with that in the bulk. Thin films have many applications such as corrosion resistant coating, microelectronics and integrated circuits, etc. Vinci and

Vlassak [1] reviewed the mechanical behavior of thin films, and proposed new experimental techniques to measure thin film properties. Zhao *et al.* [2] introduced a method that utilizes only the loading curves of an indentation test to extract the elastoplastic properties of an elastic-perfectly plastic thin film as well as the plastic properties of a work hardening thin film. Pervan *et al.* [3] studied the growth mode, structural and electronic properties of ultra-thin films at room temperature by means of Auger electron spectroscopy, low energy electron diffraction and angular-resolved photoemission. Ngo *et al.* [4] investigated the stress field in a multilayer thin films-substrate system subjected to non-uniform temperature and misfit strains based on an extension of the classical Stoney formula.

Contact mechanics problem of a surface-loaded layer based on a rigid base has a wide range of practical applications in the field of microelectronics, nano-indentation, and surface coating. Chen *et al.* [5] studied the mechanical properties of thin film-substrate systems by nano-indentation, considering the effects of thickness and different coating-substrate

✉ *Corresponding Author: Ali Oveysi Sarabi
Email: alioveysisarabi@gmail.com
Tel.: (+98) 9184744982
Fax: (+98) 8345127477

combinations. They found that the classical plasticity theory cannot predict the experimental results, even considering the indenter tip curvature. Li *et al.* [6] investigated the influence of contact geometry, including the round tip of the indenter and the roughness of the specimen, on hardness behavior for elastic-plastic materials by means of finite element simulation. Dhaliwal and Rau [7,8] reduced the axisymmetric Boussinesq problem of an elastic layer lying over an elastic half-space to a Fredholm integral equation that was solved numerically to obtain the elastic field.

Nowadays, a film can be made as thin as few nanometers using modern processing technologies. Yasumoto and Tomimasu [9] proposed a novel method for thin film fabrication using the mid-infrared free electron laser having a tunable wavelength. Itaka *et al.* [10] demonstrated combinatorial approach in investigation of organic thin film fabrication. Through high ratio of surface to volume of ultra-thin films, it is necessary to consider surface stress effects, which is usually neglected in the classical mechanics. Gurtin and Murdoch [11,12] proposed a generic theoretical approach based on continuum mechanics concepts to account the surface energy. The Gurtin-Murdoch surface stress model has recently been used to consider surface stress effects in modern contact problems. Mogilevskaya *et al.* [13] analyzed a two-dimensional problem of multiple interacting circular nanoinhomogeneities based on the Gurtin-Murdoch model. Li *et al.* [14] examined the effect of surface stress on stress concentration near a spherical void in an elastic medium using Gurtin-Murdoch continuum elasticity. He and Lim [15] derived surface Green function for incompressible, elastically isotropic half-space coupled with surface stress by using double Fourier transform technique and Gurtin-Murdoch model. Gordelij *et al.* [16] used the generalized Gurtin-Murdoch model for a two-dimensional, transient, uncoupled thermoelastic problem of an infinite medium with a circular nano-scale cavity. Based on the surface elasticity theory, Koguchi [17] presented Green's functions for anisotropic elastic half-space using Stroh's formulas. Bar On *et al.* [18] developed a continuum model for nanobeams, including both surface effects and material heterogeneity. A comparison between continuum and atomistic solutions revealed differences. This result, originated from local transition effects in the neighborhood of strong non-uniformities. Shen and

Hu [19] proposed an elastic enthalpy variational principle for nanosized dielectrics concerning with the flexoelectric effect, the surface effects and the electrostatic force where surface effects contain the effects of both surface stress and surface polarization.

According to the above literature review, it can be concluded that developed solutions based on Gurtin-Murdoch continuum elasticity accounting for the surface stress effects is necessary to study nanofilms. In this work, a general two-dimensional problem for an isotropic elastic ultra-thin film bonded to a rigid substrate and subjected to inclined concentrated loading is considered in the presence of surface stress effects.

EXPERIMENTAL

Fundamental Equations

The constitutive relations of the bulk material relating non-zero stresses to the corresponding strains can be expressed as

$$\sigma_{ij} = 2\mu\varepsilon_{ij} + \lambda\delta_{ij}\varepsilon_{kk} \quad (1)$$

where σ_{ij} and ε_{ij} denote, in sequence, components of displacement and stress, δ_{ij} is the usual Kronecker delta, μ and λ are the Lamé constants of the bulk material.

According to the Gurtin-Murdoch continuum model, surface constitutive relation can be obtained as

$$\sigma_{\alpha\beta}^0 = \tau_0\delta_{\alpha\beta} + (\lambda_0 + \tau_0)\varepsilon_{\gamma\gamma}\delta_{\alpha\beta} + 2(\mu_0 - \tau_0)\varepsilon_{\alpha\beta} \quad (2)$$

where τ_0 is the surface residual stress without constraint; λ_0 and μ_0 are surface Lamé constants or surface elastic constants.

Note that the surface stress is a second rank tensor in tangent plane of the surface, so α and β take integers 1 or 2.

Non-Classical Solution for Displacement and Stress Components

Non-Classical Solution with Finite Thickness of Layer:

The nanofilm considered herein is an elastic layer with finite thickness subjected to external inclined point loading on the surface. A Cartesian coordinate system (x_1, x_2, x_3) is introduced as shown in Fig. 1.

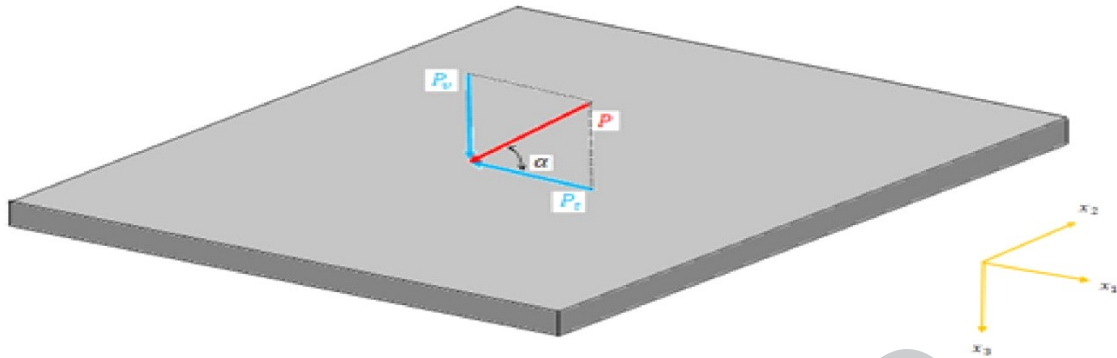


Fig. 1: Nanofilm subjected to inclined point load.

The displacement and stress components are indicated by u_i and σ_{ij} , respectively. The general solution for these components of displacement and stress for a two-dimensional elastic layer can be expressed using Fourier integral transforms as [20,21]

$$u_1 = \frac{1}{4\pi\mu} \int_{-\infty}^{\infty} \left\{ \left[A\eta - B \left(\frac{\lambda+2\mu}{\lambda+\mu} \frac{|\eta|}{\eta} - x_3|\eta| \right) \right] e^{-x_3|\eta|} + \left[C\eta + D \left(\frac{\lambda+2\mu}{\lambda+\mu} \frac{|\eta|}{\eta} + x_3|\eta| \right) \right] e^{x_3|\eta|} \right\} e^{-ix_1\eta} d\eta$$

$$u_3 = \frac{1}{4\pi\mu} \int_{-\infty}^{\infty} \left\{ \left[A|\eta| + B \left(\frac{\mu}{\lambda+\mu} + x_3|\eta| \right) \right] e^{-x_3|\eta|} + \left[-C|\eta| + D \left(\frac{\mu}{\lambda+\mu} - x_3|\eta| \right) \right] e^{x_3|\eta|} \right\} e^{-ix_1\eta} d\eta$$

$$\sigma_{11} = \frac{1}{2\pi} \int_{-\infty}^{\infty} \left\{ \left[A\eta^2 - B(2|\eta| - x_3\eta^2) \right] e^{-x_3|\eta|} + \left[C\eta^2 + D(2|\eta| + x_3\eta^2) \right] e^{x_3|\eta|} \right\} e^{-ix_1\eta} d\eta$$

$$\sigma_{33} = -\frac{1}{2\pi} \int_{-\infty}^{\infty} \eta^2 \left\{ (A + Bx_3) e^{-x_3|\eta|} + (C + Dx_3) e^{x_3|\eta|} \right\} e^{-ix_1\eta} d\eta$$

$$\sigma_{13} = \frac{i}{2\pi} \int_{-\infty}^{\infty} \eta \left\{ \left[A|\eta| + B(1 - x_3|\eta|) \right] e^{-x_3|\eta|} + \left[C|\eta| + D(1 + x_3|\eta|) \right] e^{x_3|\eta|} \right\} e^{-ix_1\eta} d\eta \quad (3)$$

Where $\eta = \sqrt{-1}$, and A, B, C, D are the arbitrary coefficients which can be determined by boundary conditions.

$$\sigma_{33}|_{x_3=0} = -p_v(x_1) \quad (4-a)$$

$$\sigma_{13}|_{x_3=0} = -\left[p_t(x_1) + (2\mu_0 + \lambda_0) \frac{d^2 u_1}{dx_1^2} \right] \quad (4-b)$$

$$u_1|_{x_3=h} = 0 \quad (4-c)$$

$$u_3|_{x_3=h} = 0 \quad (4-d)$$

By applying Fourier integral transform to equations (4) and substituting equation (3), the following equations can be obtained:

$$A + C = \frac{P_v}{\eta^2} \quad (5-a)$$

$$B + D - (A - C)|\eta| - \frac{2\mu_0 + \lambda_0}{2\mu} \left[\frac{\lambda + 2\mu}{\lambda + \mu} (D - B)|\eta| + (A + C)\eta^2 \right] = \frac{P_t}{i\eta} \quad (5-b)$$

$$\left[\frac{\mu}{\lambda + \mu} B + (A + Bh)|\eta| \right] e^{-h|\eta|} + \left[\frac{\mu}{\lambda + \mu} D - (C + Dh)|\eta| \right] e^{h|\eta|} = 0 \quad (5-c)$$

$$\left[-\frac{\lambda + 2\mu}{\lambda + \mu} B + (A + Bh)|\eta| \right] e^{-h|\eta|} + \left[\frac{\lambda + 2\mu}{\lambda + \mu} D + (C + Dh)|\eta| \right] e^{h|\eta|} = 0 \quad (5-d)$$

where P_v and P_t are the Fourier integral transforms of $p_v(x_1)$ and $p_t(x_1)$, respectively.

The coefficients A, B, C and D can be obtained by solving the equations (5) as

$$A = \frac{A' + iA''}{H}, \quad B = \frac{B' + iB''}{H}, \quad C = \frac{C' + iC''}{H}, \quad D = \frac{D' + iD''}{H} \quad (6)$$

$$A' = \frac{P_v}{2\eta^2} \left\{ (\lambda + 3\mu) \left[(1 + \psi|\eta|) e^{2h|\eta|} - \psi|\eta| \right] + 2h\eta^2(\lambda + \mu)(\psi + h) - \frac{2(\lambda + \mu)^2}{\lambda + 2\mu} \psi h^2 |\eta|^3 - 2(\lambda + \mu)h|\eta| + \frac{\lambda^2 + 4\lambda\mu + 5\mu^2}{\lambda + \mu} \right\}$$

$$A'' = -\frac{P_t}{|\eta|\eta} \left[\frac{\mu(\lambda + 2\mu)}{\lambda + \mu} + (\lambda + \mu)h^2\eta^2 \right]$$

$$\begin{aligned}
 B' &= \frac{P_v}{2|\eta|} \left\{ (\lambda + 3\mu) \left[\left(1 + \frac{\lambda + \mu}{\lambda + 2\mu} \psi |\eta| \right) e^{2h|\eta|} - \frac{\lambda + \mu}{\lambda + 2\mu} \psi |\eta| \right] \right. \\
 &\quad \left. + \frac{2(\lambda + \mu)^2}{\lambda + 2\mu} \psi h \eta^2 + (\lambda + \mu)(1 - 2h|\eta|) \right\} \\
 B'' &= \frac{P_t}{2\eta} [(\lambda + 3\mu)e^{2h|\eta|} + (\lambda + \mu)(1 + 2h|\eta|)] \\
 C' &= \frac{P_v}{2\eta^2} \left\{ (\lambda + 3\mu) [(1 - \psi |\eta|) e^{-2h|\eta|} + \psi |\eta|] \right. \\
 &\quad \left. + 2h\eta^2 (\lambda + \mu)(\psi + h) + \frac{2(\lambda + \mu)^2}{\lambda + 2\mu} \psi h^2 |\eta|^3 \right. \\
 &\quad \left. + 2(\lambda + \mu)h|\eta| + \frac{\lambda^2 + 4\lambda\mu + 5\mu^2}{\lambda + \mu} \right\} \\
 C'' &= \frac{P_t}{|\eta|\eta} \left[\frac{\mu(\lambda + 2\mu)}{\lambda + \mu} + (\lambda + \mu)h^2 \eta^2 \right] \\
 D' &= -\frac{P_v}{2|\eta|} \left\{ (\lambda + 3\mu) \left[\left(1 - \frac{\lambda + \mu}{\lambda + 2\mu} \psi |\eta| \right) e^{-2h|\eta|} + \right. \right. \\
 &\quad \left. \left. \frac{\lambda + \mu}{\lambda + 2\mu} \psi |\eta| \right] + \frac{2(\lambda + \mu)^2}{\lambda + 2\mu} \psi h \eta^2 + (\lambda + \mu)(1 + 2h|\eta|) \right\} \\
 D'' &= \frac{P_t}{2\eta} [(\lambda + 3\mu)e^{-2h|\eta|} + (\lambda + \mu)(1 - 2h|\eta|)] \\
 H &= (\lambda + 3\mu) [\cosh(2h\eta) + \psi \eta \sinh(2h\eta)] + \\
 &\quad 2h\eta^2 (\lambda + \mu)(\psi + h) + \frac{\lambda^2 + 4\lambda\mu + 5\mu^2}{\lambda + \mu}
 \end{aligned}$$

and $\psi = \frac{(2\mu_0 + \lambda_0)(2\mu + \lambda)}{\lambda + \mu}$ is a constant with the dimension of length. In the absence of surface stress effects, the value of ψ will be vanished and the solution will be reduced to the classical one.

Non-Classical Solution with Infinite Thickness of Layer

When the value of thickness of a nanofilm is so larger than its other dimensions, it can be assumed that h approaches infinity, and the above solution will be reduced to the following closed-form

$$\begin{aligned}
 u_1 &= (u_1)_v + (u_1)_t \\
 u_3 &= (u_3)_v + (u_3)_t \\
 \sigma_{11} &= (\sigma_{11})_v + (\sigma_{11})_t \\
 \sigma_{33} &= (\sigma_{33})_v + (\sigma_{33})_t \\
 \sigma_{13} &= (\sigma_{13})_v + (\sigma_{13})_t
 \end{aligned} \tag{7}$$

where

$$\begin{aligned}
 (u_1)_v &= \frac{P_v}{2\pi} \left[-\frac{1}{\lambda + \mu} \text{Arctan} \frac{x_1}{x_3} + \frac{x_1 x_3}{\mu(x_1^2 + x_3^2)} + \frac{\psi}{\lambda + \mu} \int_0^\infty \frac{e^{-x_3 \eta} \sin(x_1 \eta)}{1 + \psi \eta} d\eta \right. \\
 &\quad \left. + \frac{x_3}{\lambda + 2\mu} \left(\int_0^\infty \frac{e^{-x_3 \eta} \sin(x_1 \eta)}{1 + \psi \eta} d\eta - \frac{x_3}{x_1^2 + x_3^2} \right) \right] \\
 (u_1)_t &= \frac{P_t}{2\pi} \left[-\frac{\lambda + 2\mu}{\mu(\lambda + \mu)} \int_0^\infty \frac{e^{-x_3 \eta} \cos(x_1 \eta)}{\eta} d\eta + \right. \\
 &\quad \frac{x_3}{\mu} \int_0^\infty e^{-x_3 \eta} \cos(x_1 \eta) d\eta - \frac{\psi(\lambda + 2\mu)}{\mu(\lambda + 2\mu)} \int_0^\infty \frac{e^{-x_3 \eta} \cos(x_1 \eta)}{1 + \psi \eta} d\eta \\
 &\quad \left. + \frac{x_3}{\mu} \left(-\int_0^\infty \frac{e^{-x_3 \eta} \cos(x_1 \eta)}{1 + \psi \eta} d\eta + \frac{x_3}{x_1^2 + x_3^2} \right) \right]
 \end{aligned}$$

$$\begin{aligned}
 (u_3)_v &= \frac{P_v}{2\pi} \left[\frac{\lambda + 2\mu}{\mu(\lambda + \mu)} \int_0^\infty \frac{e^{-x_3 \eta} \cos(x_1 \eta)}{\eta} d\eta + \frac{x_3}{\mu} \int_0^\infty e^{-x_3 \eta} \cos(x_1 \eta) d\eta \right. \\
 &\quad \left. - \frac{\psi \mu}{(\lambda + \mu)(\lambda + 2\mu)} \int_0^\infty \frac{e^{-x_3 \eta} \cos(x_1 \eta)}{1 + \psi \eta} d\eta \right. \\
 &\quad \left. + \frac{x_3}{\lambda + 2\mu} \left(\int_0^\infty \frac{e^{-x_3 \eta} \cos(x_1 \eta)}{1 + \psi \eta} d\eta - \frac{x_3}{x_1^2 + x_3^2} \right) \right] \\
 (u_3)_t &= \frac{P_t}{2\pi} \left[\frac{1}{\lambda + \mu} \text{Arctan} \frac{x_1}{x_3} + \frac{x_1 x_3}{\mu(x_1^2 + x_3^2)} - \frac{\psi}{\lambda + \mu} \int_0^\infty \frac{e^{-x_3 \eta} \sin(x_1 \eta)}{1 + \psi \eta} d\eta \right. \\
 &\quad \left. + \frac{x_3}{\lambda + 2\mu} \left(\int_0^\infty \frac{e^{-x_3 \eta} \sin(x_1 \eta)}{1 + \psi \eta} d\eta - \frac{x_3}{x_1^2 + x_3^2} \right) \right] \\
 (\sigma_{11})_v &= \frac{P_v}{\pi} \left\{ -\frac{2x_1^2 x_3}{(x_1^2 + x_3^2)^2} + \frac{\mu}{\lambda + 2\mu} \left[(x_3 + 2) \left(-\int_0^\infty \frac{e^{-x_3 \eta} \cos(x_1 \eta)}{1 + \psi \eta} d\eta \right) \right. \right. \\
 &\quad \left. \left. + \frac{x_3}{x_1^2 + x_3^2} \right) - \frac{x_3(x_3^2 - x_1^2)}{(x_1^2 + x_3^2)^2} \right\} \\
 (\sigma_{11})_t &= \frac{P_t}{\pi} \left[-\frac{2x_1^2}{(x_1^2 + x_3^2)^2} - \frac{2x_1 x_3^2}{(x_1^2 + x_3^2)^2} + (x_3 + 2) \left(-\int_0^\infty \frac{e^{-x_3 \eta} \sin(x_1 \eta)}{1 + \psi \eta} d\eta + \frac{x_3}{x_1^2 + x_3^2} \right) \right] \\
 (\sigma_{33})_v &= \frac{P_v}{\pi} \left\{ -\frac{2x_3^2}{(x_1^2 + x_3^2)^2} + \frac{\mu}{\lambda + 2\mu} \left[x_3 \left(\int_0^\infty \frac{e^{-x_3 \eta} \cos(x_1 \eta)}{1 + \psi \eta} d\eta - \frac{x_3}{x_1^2 + x_3^2} \right) + \frac{x_3(x_3^2 - x_1^2)}{(x_1^2 + x_3^2)^2} \right] \right\} \\
 (\sigma_{33})_t &= \frac{P_t}{\pi} \left[x_3 \left(\int_0^\infty \frac{e^{-x_3 \eta} \cos(x_1 \eta)}{1 + \psi \eta} d\eta - \frac{x_3}{x_1^2 + x_3^2} \right) \right] \\
 (\sigma_{13})_v &= \frac{P_v}{\pi} \left\{ -\frac{2x_1 x_3^2}{(x_1^2 + x_3^2)^2} + \frac{\mu}{\lambda + 2\mu} \left[(x_3 + 1) \left(-\int_0^\infty \frac{e^{-x_3 \eta} \sin(x_1 \eta)}{1 + \psi \eta} d\eta + \frac{x_3}{x_1^2 + x_3^2} \right) - \frac{2x_1 x_3^2}{(x_1^2 + x_3^2)^2} \right] \right\} \\
 (\sigma_{13})_t &= \frac{P_t}{\pi} \left[-\frac{2x_1^2 x_3}{(x_1^2 + x_3^2)^2} + (x_3 + 1) \left(-\int_0^\infty \frac{e^{-x_3 \eta} \sin(x_1 \eta)}{1 + \psi \eta} d\eta + \frac{x_3}{x_1^2 + x_3^2} \right) - \frac{x_3(x_3^2 - x_1^2)}{(x_1^2 + x_3^2)^2} \right]
 \end{aligned}$$

If $\psi = 0$, the solution obviously reduces to the classical elasticity solution.

RESULTS AND DISCUSSION

Numerical Results

As it was shown in the previous sections, a closed-form solution for the case of a nanofilm with finite value of thickness cannot be obtained due to the complexity of the integrands. However, numerical technique is used to calculate the elastic field of a layer with finite thickness. In this section, selected numerical results are presented for Nickel [1 1 1] surface to indicate the influence of surface stress effects on the elastic field of ultra-thin layer subjected to inclined point loading. The material surface constants corresponding to Nickel surface can be obtained from atomistic simulations [22,23], which are: $\mu_0 = 1.655 \text{ N/m}$, $\lambda_0 = 1.247 \text{ N/m}$, $\tau_0 = 0.1154 \text{ N/m}$. The bulk elastic

constants for Nickel are: $\mu = 76 \text{ GPa}$, $\lambda = 126.2 \text{ GPa}$ [24]. In the following numerical results for the case of finite thickness of layer, it is taken that $h = 40\psi$. The non-dimensional coordinates are used to show the numerical results as: $\bar{x}_1 = x_1/\psi$, $\bar{x}_3 = x_3/\psi$, $\bar{h} = h/\psi$.

Depicted in Figs. 2 and 3 are the distributions of the surface displacements of the nanofilm due to inclined point loading with angle of $\alpha = 45^\circ$ at different depths of the layer. It can be seen that the surface stress effects have significant influence on the distribution of displacement especially at lower depth of the layer and make the layer stiffer than the classic case. However, both in classical and non-classical solutions displacements decrease at lower depth of the layer.

Figs. 4-6 show the stress profiles of the nanofilm at different depths of the layer under inclined point

load with angle of . The remarkable influence of surface stress effects on the distribution of stress is found clearly. Also, the stiffening behavior through surface stress effects observed previously for displacement profiles can be seen for the distribution of stresses in all cases of depth of the layer.

Figs. 7-11 illustrate the influence of angle of loading on the distribution of different components of displacement and stress along the x_1 axis. It is found that with increase of angle of loading (approaching to vertical point load) surface stress effects are more important and stiffening the layer due to these effects is quite significant for upper values of α . So, it can be concluded that the surface stress effects have more remarkable influence on the displacement and stress profiles for the case of vertical point load in comparison with the horizontal point load.

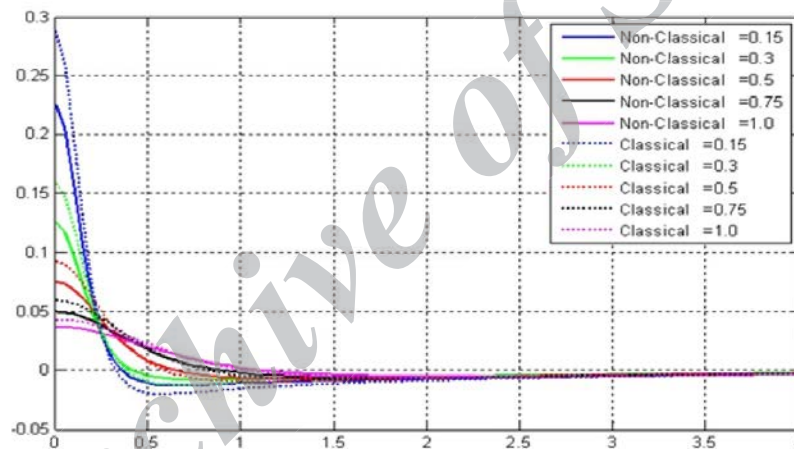


Fig. 2: Distribution of nondimensional horizontal displacement at different depths of the layer along the x_1 axis.

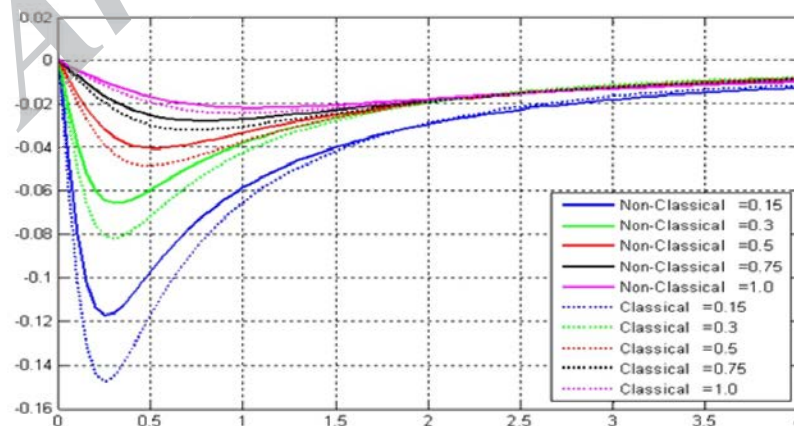


Fig. 3: Distribution of nondimensional vertical displacement at different depths of the layer along the x_1 axis.

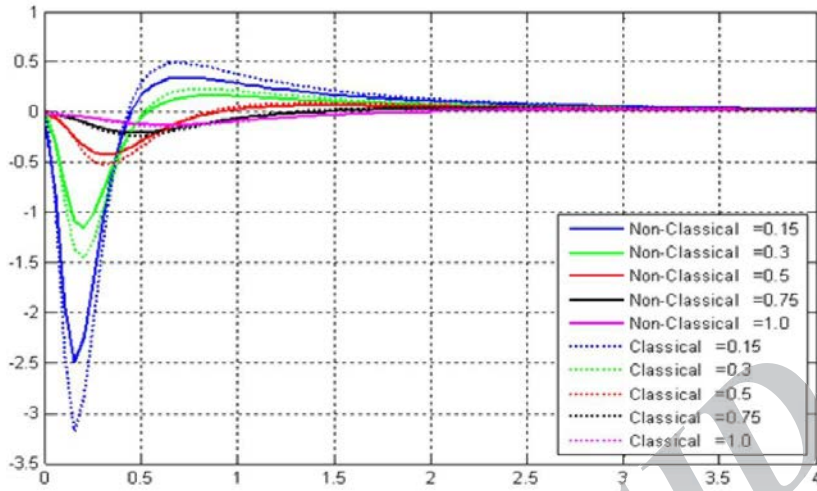


Fig. 4: Distribution of nondimensional horizontal stress at different depths of the layer.

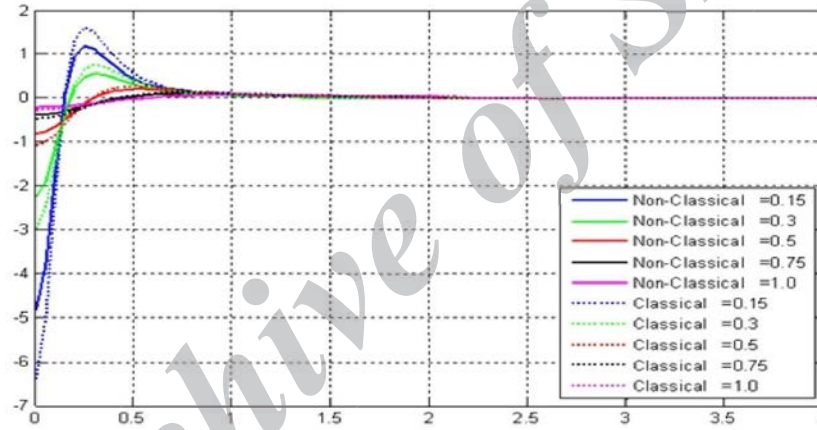


Fig. 5: Distribution of nondimensional vertical stress at different depths of the layer along the axis.

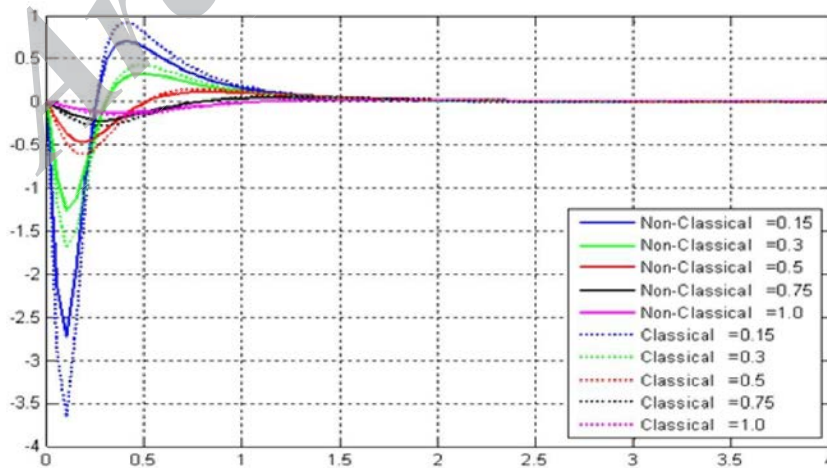


Fig. 6: Distribution of nondimensional shear stress at different depths of the layer along the axis.

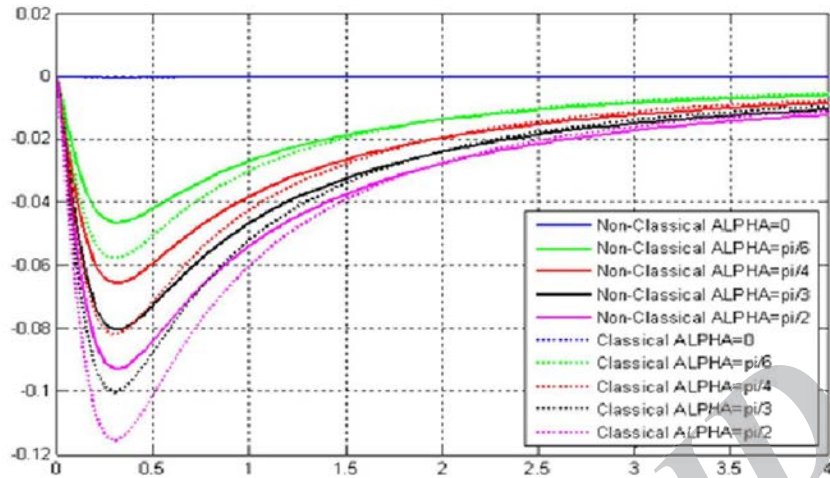


Fig. 7: Variation of nondimensional horizontal displacement profile versus the angle of loading along the axis.

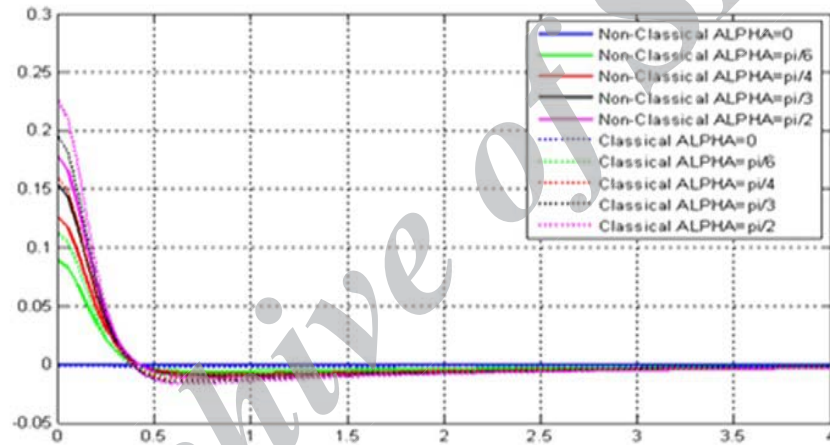


Fig. 8: Variation of nondimensional vertical displacement profile versus the angle of loading along the axis.

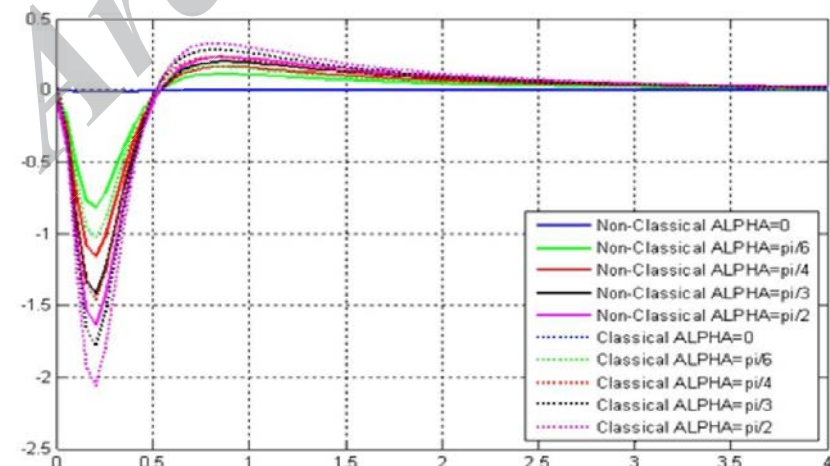


Fig. 9: Variation of nondimensional horizontal stress profile versus the angle of loading along the x_2 axis ($\bar{x}_2 = 0.3$).

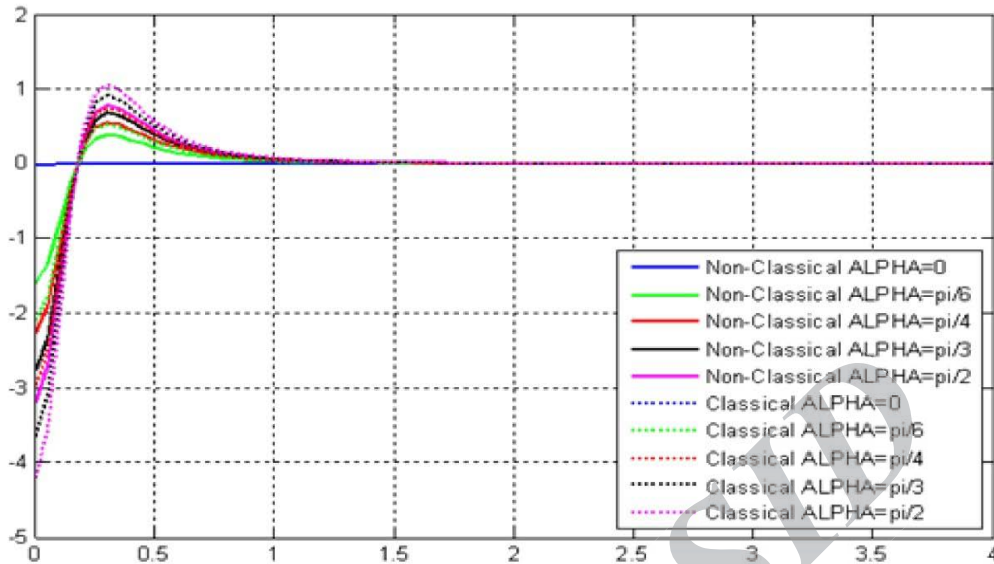


Fig. 10: Variation of nondimensional vertical stress profile versus the angle of loading along the x_1 axis ($\bar{x}_2 = 0.3$).

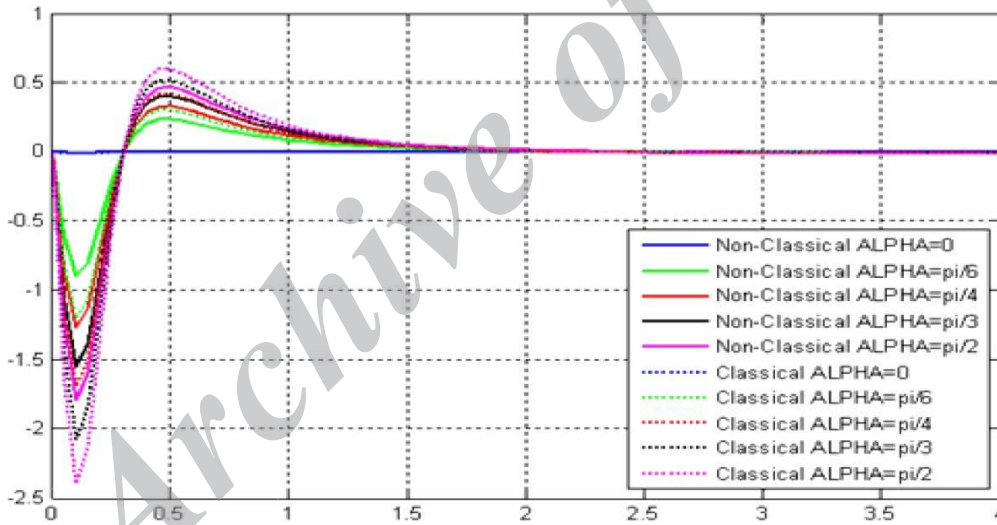


Fig. 11: Variation of nondimensional shear stress profile versus the angle of loading along the x_1 axis ($\bar{x}_2 = 0.3$).

Convergence of the numerical results

In Tables 1 and 2, the convergence criterion of some of the selected numerical results is examined. It is observed from these tables that the convergence is achieved rapidly.

In Table 1, the value of non-dimensional displacement components are given for the layer with different thicknesses and $\bar{x}_1 = 0.5$. Table 2 shows the values of non-dimensional stress components at

different depths of the layer with the layer thickness $\bar{h} = 40\psi$ and . The Gauss quadrature technique is used to calculate numerical integration. In each iteration, the number of intervals has increased from the previous one to decrease the error of approximation. This pattern of convergence of the numerical technique reflects its efficiency and accuracy.

Table 1: Convergence of non-classical results for nondimensional stress components.

Number of Iteration	$\alpha = 45^\circ$			$\alpha = 90^\circ$		
	$\frac{\psi\sigma_{11}}{P}$	$\frac{\psi\sigma_{33}}{P}$	$\frac{\psi\sigma_{13}}{P}$	$\frac{\psi\sigma_{11}}{P}$	$\frac{\psi\sigma_{33}}{P}$	$\frac{\psi\sigma_{13}}{P}$
1	0.08550725	0.35743637	0.30757791	0.08609984	0.47411344	0.43233865
2	0.08793392	0.36758031	0.31630688	0.08854333	0.48756864	0.44460830
3	0.08852460	0.37004947	0.31843162	0.08913811	0.49084380	0.44759488
4	0.08867139	0.37066306	0.31895966	0.08928593	0.49165768	0.44833705
5	0.08870803	0.37081623	0.31909147	0.08932283	0.49186085	0.44852232
6	0.08871719	0.37085451	0.31912441	0.08933205	0.49191162	0.44856862
7	0.08871948	0.37086408	0.31913264	0.08933436	0.49192431	0.44858020
8	0.08872005	0.37086647	0.31913470	0.08933494	0.49192749	0.44858310
9	0.08872019	0.37086707	0.31913522	0.08933508	0.49192829	0.44858383
10	0.08872024	0.37086727	0.31913539	0.08933513	0.49192855	0.44858407

Table 2: Convergence of non-classical results for nondimensional displacement components.

Number of Iteration	$\alpha = 45^\circ$		$\alpha = 90^\circ$	
	$\frac{\mu_0 u_1}{\psi P}$	$\frac{\mu_0 u_3}{\psi P}$	$\frac{\mu_0 u_1}{\psi P}$	$\frac{\mu_0 u_3}{\psi P}$
1	-0.05765540	-0.01167109	-0.08171989	-0.01202427
2	-0.05929164	-0.01200231	-0.08403908	-0.01236552
3	-0.05968992	-0.01208293	-0.08460360	-0.01244859
4	-0.05978890	-0.01210297	-0.08474389	-0.01246923
5	-0.05981361	-0.01210798	-0.08477891	-0.01247438
6	-0.05981979	-0.01210923	-0.08478766	-0.01247567
7	-0.05982134	-0.01210955	-0.08478985	-0.01247601
8	-0.05982173	-0.01210968	-0.08479043	-0.01247609
9	-0.05982182	-0.01210976	-0.08479056	-0.01247613
10	-0.05982185	-0.01210979	-0.08479061	-0.01247615

CONCLUSION

This work presents a non-classical continuum model accounting for surface stress effects based on Gurtin-Murdoch elasticity theory to analyze the elastic field of nanofilms subjected to inclined point load. The analysis is performed assuming both finite and infinite thickness of layer. Selected numerical results are presented to demonstrate the salient features of the response of the layer to assess the influence of surface stress effects. The governing equations are developed for inclined point load with arbitrary value of angle of loading. It is shown that close form analytical solution can be obtained for the case of infinite thickness of the layer. The present non-classical solution shows that the surface elastic properties make the material stiffer than the classical case through consideration of surface stress effects.

It is found that in the lower depths of the layer, the surface stress effects have more significant influence on the displacement and stress profiles and have little influence on the base of the layer. Also, it is shown that by approaching the case of vertical point load (by increasing the value of α), the influence of surface stress effects is quiet strong compared to horizontal point loading.

REFERENCES

- [1] Vinci R. P., Vlassak J. J., (1996), Mechanical behavior of thin films. *Annual Rev. Mater. Sci.* 26: 431-462.
- [2] Zhao M., Xiang Y., Xu J., Ogasawara N., Chiba N., Chen X., (2008), Determining mechanical properties of thin films from the loading curve of nanoindentation testing. *Thin Solid Films.* 516: 7571-7580.
- [3] Pervan P., Valla T., Milun M., (1998), Structural and

- electronic properties of vanadium ultra-thin film on Cu(100). *Surf. Sci.* 397: 270-277.
- [4] Ngo D., Feng X., Huang Y., Rosakis A. J., (2008), Multilayer thin films/substrate system with variable film thickness subjected to non-uniform misfit strains. *Acta Mater.* 56: 5322-5328.
- [5] Chen S. H., Liu L., Wang T. C., (2007), Small scale, grain size and substrate effects in nano-indentation experiment of film-substrate systems. *Int. J. Solids and Struct.* 44: 4492-4504.
- [6] Li M., Chen W., Cheng Y., Cheng C., (2009), Influence of contact geometry on hardness behavior in nano-indentation. *Vacuum.* 84: 315-320.
- [7] Dhaliwal R. S., Rau I. S., (1970), The axisymmetric boussinesq problem for a thick elastic layer under a punch of arbitrary profile. *Int. J. Eng. Sci.* 8: 843-856.
- [8] Dhaliwal R. S., Rau I. S., (1972), Further consideration on the axisymmetric boussinesq problem. *Int. J. Eng. Sci.* 10: 659-663.
- [9] Yasumoto M., Tomimasu T., (2002), A proposed novel method for thin-film fabrication assisted by mid-infrared free electron laser, Nuclear Instruments and Methods in Physics Research Section A: Accelerators, Spectrometers. *Detec. Assoc. Equip.* 480: 92-97.
- [10] Itaka K., Yamashiro M., Yamaguchi J., Yaginuma S., Haemori M., Koinuma H., (2006), Combinatorial approach to the fabrication of organic thin films. *App. Surf. Sci.* 252: 2562-2567.
- [11] Gurtin M. E., Murdoch A. I., (1975), A continuum theory of elastic material surface. *Arch. Ratio. Mech. Anal.* 57: 291-323.
- [12] Gurtin M. E., Murdoch A. I., (1978), Surface stress in solids. *Int. J. Solids and Struct.* 14: 431-440.
- [13] Mogilevskaya S. G., Crouch S. L., Stolarski H. K., (2008), Multiple interacting circular nano-inhomogeneities with surface/interface effects. *J. Mech. Phys. Solids.* 56: 2298-2327.
- [14] Li Z. R., Lim C. W., He L. H., (2006), Stress concentration around a nanoscale spherical cavity in elastic media: effects of surface stress. *Europ. J. Mech. A.:Solids.* 25: 260-270.
- [15] He L. H., Lim C. W., (2006), Surface Green function for a soft elastic half-space: influence of surface stress. *Int. J. Solids and Struct.* 43: 132-143.
- [16] Gordeliy E., Mogilevskaya S. F., Crouch S. L., (2009), Transient thermal stresses in a medium with a circular cavity with surface effects. *Int. J. Solids and Struct.* 46: 1834-1848.
- [17] Koguchi H., (2008), Surface Green function with surface stresses and surface elasticity using Stroh's formalism. *J. Appl. Mech. Transact. ASME.* 75: 061014.
- [18] Bar On B., Altus E., Tadmor E. B., (2010), Surface effects in non-uniform nanobeams: continuum vs. atomistic modeling. *Int. J. Solids and Struct.* 47: 1243-1252.
- [19] Shen S., Hu S., (2010), A theory of flexoelectricity with surface effect for elastic dielectrics. *J. Mech. Phys. Solids.* 58: 665-677.
- [20] Sneddon I. N., (1951), Fourier transforms, McGraw-Hill, New York, Springer.
- [21] Selvadurai A. P. S., (2000), Partial differential equations in mechanics, New York, Springer.
- [22] Miller R. E., Shenoy V. B., (2000), Size-dependent elastic properties of nanosized structural elements. *Nanotech.* 11: 139-147.
- [23] Shenoy V. B., (2005), Atomistic calculations of elastic properties of metallic fcc crystal surfaces. *Phys. Rev. B.* 71: 094104.
- [24] Meyers M. A., Chawla K. K., (1999), Mechanical behavior of materials, Prentice-Hall, NJ.

How to cite this article: (Vancouver style)

Oveysi Sarabi A. and Ghanbari A., (2015), Examining and calculation of non-classical in the solutions to the true elastic cable under concentrated loads in nanofilm. *Int. J. Nano Dimens.* 6(5): 463-472.

DOI: 10.7508/ijnd.2015.05.003

URL: http://ijnd.ir/article_15183_1117.html